RESEARCH PAPER

Development and Characterization of Bidara (Ziziphus mauritiana) Essential Oil-Loaded Solid Lipid Nanoparticles with Evaluation of Antioxidant Activity and Short-Term Storage Stability

Muhammad Faris Bin Khairul Anuar[1], Samah Hamed Almurisi[2], Syed Mahmood[3], Rahul Pal[4], Fawaz Alheibshy[5], Nasrin E. Khalifa[5], Syed Haroon Khalid[1,6*], Khater AL-Japairai[1,7*]

[1]Department of Pharmaceutical Technology, Faculty of Pharmacy, Universiti Teknologi MARA, Puncak Alam 42300, Selangor, Malaysia

[2]Department of Pharmaceutical Technology, School of Pharmacy, IMU University, Kuala Lumpur 57000, Malaysia

[3]Department of Pharmaceutical Technology, Faculty of Pharmacy, Universiti Malaya, Kuala Lumpur 50603, Malaysia

[4]University Institute of Pharma Sciences (UIPS), Chandigarh University, Mohali, 140413, Punjab, India

[5]Department of Pharmaceutics, College of Pharmacy, University of Hail, 2240, Hail, Saudi Arabia

[6]Department of Pharmaceutics, Faculty of Pharmaceutical Sciences, Government College University Faisalabad, 38000, Faisalabad Pakistan

[7]Innovative Drug Development and Delivery Research Group (InDeeD), Faculty of Pharmacy, UiTM Cawangan Selangor, Bandar Puncak Alam, 42300, Selangor, Malaysia

***Corresponding authors:**

Khater AL-Japairai; khater@uitm.edu.my , ORCID: https://orcid.org/0000-0002-1426-9575

Syed Haroon Khalid; syedharoonkhalid@gcuf.edu.pk

Abstract

Bidara (Ziziphus mauritiana) essential oil exhibits potential biological properties; however, its therapeutic application is constrained by inadequate stability and high volatility. This research focused on creating and enhancing Bidara essential oil-loaded solid lipid nanoparticles (BEO-SLNs) to enhanced the stability and biological efficacy of the essential oil. Gas chromatography-mass spectrometry (GC-MS) was done to evaluate the bioactive compound of Bidara essential oil. BEO-SLNs were synthesized utilizing a combination of high-shear homogenization and ultrasonication with various ratios of glyceryl monostearate (GMS) to essential oil. The formulations were evaluated according to physical appearance, particle size (PS), polydispersity index (PDI), zeta potential (ZP), encapsulation efficiency (EE%), loading capacity (LC%), surface morphology by scanning electron microscopy (SEM). Then the antioxidant activity was evaluated by DDPH scavenging assay and storage stability at room temperature. Gas chromatography-mass spectrometry (GC-MS) analysis revealed carvacrol (63.21%) as the primary component of Bidara essential oil. The developed BEO-SLNs showed particle sizes between 87.58 and 98.30 nm, with PDI values under 0.25 and zeta potential values ranging from −17.0 to −39.4 mV. Encapsulation efficiency stayed consistently high across every formulation (97.34-99.54%), whereas loading capacity diminished as lipid content increased (18.13-47.53%). SEM analysis revealed predominantly spherical to irregularly spherical nanoparticles with rough surface morphology and slight particle aggregation. Of all the formulations, SLN1 showed the most advantageous physicochemical characteristics and displayed 72.11± 0.1% DPPH radical scavenging activity. Stability studies indicated that the formulations preserved acceptable physicochemical properties after 30 days of storage. In summary, BEO-SLNs were effectively created with excellent encapsulation efficiency, good stability, and notable antioxidant activity, suggesting their promise as a viable nanocarrier system for improving the therapeutic use of Bidara essential oil.

Keywords: Solid lipid nanoparticle, Bidara essential oil, high speed homogenization, ultrasonication, antioxidant, stability study.

How to cite this article: Muhammad Faris Bin Khairul Anuar1 Samah Hamed Almurisi2 Syed Mahmood3 Rahul Pal4 Fawaz Alheibshy5 Nasrin E. Khalifa5 Syed Haroon Khalid16* Khater AL-Japairai17*. Development and Characterization of Bidara (Ziziphus mauritiana) Essential Oil-Loaded Solid Lipid Nanoparticles with Evaluation of Antioxidant Activity and Short-Term Storage Stability. Int J Drug Deliv Technol. 2026;16(90s):2163-2176. DOI: 10.25258/ijddt.16.90s.218.

Introduction

Ziziphus mauritiana Lam. is a member of the Rhamnaceae family, which comprises a diverse range of flowering plants including shrubs and small trees commonly found in tropical and subtropical areas (1). The genus Ziziphus Mill. is a widely acknowledged group within this family, consisting of about 50–90 recognized species based on different taxonomic classifications, and is found in Asia, Africa, and certain regions of the Americas (2). Ziziphus mauritiana, commonly known as Indian jujube or Chinese apple have traditionally been utilized for ages in traditional medicine to address numerous conditions, such as inflammation, fever, diabetes, skin infections, gastrointestinal issues, and

microbial infections. The extensive traditional use has attracted heightened scientific interest, resulting in significant phytochemical and pharmacological research in recent years (3). According to researcher, bidara leaves, fruit, seeds, and other parts of the plant have been utilized in traditional medicine to address a range of illnesses, as well as in various cultural rituals. Among the Malay community, bidara leaves are employed in the purification of deceased bodies, as it is believed that they aid in softening the body, enhancing skin resilience, and prolonging the decomposition process (4).

Essential oils are volatile compounds that occur naturally in aromatic and medicinal plants in concentrated forms. These oils primarily consist of lipophilic secondary metabolites like terpenes, fatty acids, alcohols, aldehydes, esters, and phenolic compounds that add to the distinct aroma and biological functions of plants (5). Factors such as extraction techniques, geographical origin, environmental conditions, and plant maturity greatly influence the chemical composition and yield of essential oils (6).The essential oil derived from Ziziphus mauritiana has attracted growing scientific attention due to its possible pharmacological and therapeutic benefits. Various sections of the plant, especially the leaves and seeds, contain volatile and semi-volatile bioactive substances linked to antioxidant, antimicrobial, anti-inflammatory, and wound-healing properties. Species in the Ziziphus genus have been extensively studied for their therapeutic significance due to their varied phytochemical composition (7). Today , a recent study reveals that the essential oil of the leaves of Ziziphus mauritiana are abundant in nutrients and bioactive substances, showing notable antimicrobial effects and in vitro cytotoxicity against MCF-7 breast cancer cell lines (8).

Even though, it has promising therapeutic potential, Bidara essential oil encounters multiple formulation challenges. Essential oils are typically vulnerable to oxidation, evaporation, and deterioration when subjected to heat, oxygen, humidity, or light. Moreover, their hydrophobic characteristics can lead to low solubility in water and restricted bioavailability, thus diminishing therapeutic efficacy (6). Therefore, innovative drug delivery systems are necessary to improve the stability and therapeutic efficacy of these bioactive components. Solid lipid nanoparticles (SLNs) are effective delivery systems composed of biodegradable solid lipids that retain their solid form at room and physiological temperatures (9). SLNs are frequently employed to improve the delivery of natural oils and bioactive compounds due to their ability to enhance stability, making them highly promising system for drug delivery that enable controlled release and offer effective protection for bioactive compounds from external factors, while also showing low toxicity and excellent biodegradability (10).

This project aims to develop and enhance solid lipid nanoparticles (SLNs) loaded with Bidara (Ziziphus mauritiana) essential oil by adjusting the amounts of glyceryl monostearate and essential oil. Then, the formulated SLNs were analysed for their physicochemical characteristics, which include visual appearance, particle size, polydispersity index, zeta potential, and encapsulation efficiency. Additionally, their antioxidant capacity was evaluated using the DPPH radical scavenging test and stability testing carried out under regulated storage conditions. The results of this research could offer perspectives on the ability of lipid-based nanocarriers to improve the stability and therapeutic efficacy of Bidara essential oil.

1.0 Materials and method

1.1 Materials

The essential oil of Bidara (*Ziziphus mauritiana)* utilized in this research was obtained through an online purchase from a Malaysian commercial vendor, SRS Aromatics Sdn. Bhd. (Malaysia), a reputable domestic producer and supplier of essential oils. Glyceryl monostearate (GMS) along with the surfactants Tween 80 (polysorbate 80) and Span 80 were sourced from the Pharmacokinetic Laboratory, Faculty of Pharmacy, Universiti Teknologi MARA (UiTM) Puncak Alam. These excipients were provided by Sigma-Aldrich, a well-known chemical firm recognized for supplying pharmaceutical-quality materials. Tween 80- and Span 80-coated solid lipid nanoparticles (SLNs) have been noted to preserve nanoparticle stability and demonstrate favourable biocompatibility, validating their appropriateness for nanoparticle formulations.

1.2 Gas chromatography coupled to mass spectrometer (GC-MS)

To determine the chemical composition of Biadara essential oil, gas chromatography coupled to mass spectrometer (GC-MS) was conducted. It was analysed using a GC-MS system (Agilent 7890A GC System coupled with MSD 5975C, United States) combined with ZB-5ms fused silica capillary column (30 m × 0.25 mm i.d., 0.50 µm film thickness). The instrument was operated with an electron ionization (EI) energy of 70 eV, an ion source temperature of 230°C, and an electron emission current of 34.6 µA. The analyser temperature was maintained at 150°C. Helium was used as the carrier gas at a constant flow rate of 1.0 mL/min. The injector and interface temperatures were set at 290°C and 360°C, respectively. The oven temperature program was initiated at 50°C and held for 1 min, followed by an increase at a rate of 6°C/min until reaching 310°C, where it was maintained for 20 min. Chemical compounds were recognized by matching their retention times and mass spectra with those found in the National Institute of Standards and Technology (NIST)

library database incorporated into the GC–MS system (11).

1.3 Preparation of Bidara Essential Oil-Loaded Solid Lipid Nanoparticles

High shear homogenization method was used to formulate Bidara essential oil-loaded solid lipid nanoparticles (BEO-SLNs). Table 1 shows the expected composition of the BEO-SLNs formulation.

Table 1 Expected Composition of Bidara Essential Oil-SLNs Formulations

Solid Lipid to Essential Oil Ratio	Solid Lipid: Glyceryl Monostearate (w/w%)	Essential Oil: Bidara Essential Oil (w/w %)	Surfactant 1: Tween 80 (w/v %)	Surfactant 2: Span 80 (w/v %)	Deionized water (w/v %)
5:5	1.0	1.0	2	2	86
6:4	1.2	0.8	2	2	86
7:3	1.4	0.6	2	2	86
7.5:2.5	1.5	0.5	2	2	86
8:2	1.6	0.4	2	2	86

The first step involved glyceryl monostearate (GMS) measured at different ratio and placed into a clean beaker .The lipid was melted at a temperature approximately at 5–10 °C higher than its melting point which is at 70°C to ensure full liquefaction of the lipid phase .Subsequently, 2% v/v Span-80 was added into the lipid phase as it is a hydrophobic surfactant (12). The Bidara essential oil was then incorporated into the molten lipid phase and gently mixed to ensure that the oil was evenly distributed with the lipid phase. At the same time, the aqueous phase was prepared by dissolving 2% v/v Tween 80, a hydrophilic surfactant in deionized water. The solution was heated to the same temperature as the molten lipid phase to prevent premature solidification during emulsification (13).

After that, hot aqueous phase was added to molten lipid phase under high-speed homogenization at 12000 rpm for 10-15 minutes utilizing a D-Series Digital Benchtop Homogenizer (PRO Scientific Inc., Oxford, USA). The resulting emulsion was further ultrasonicated for 15 minutes at 30 kHz by employing a probe sonicator, which is Ultrasonic Processors 500W (Sigma-Aldrich, United Kingdom) to further reduce the particle size. Finally, the nanoemulsion was immediately cooled at room temperature with an ice bath to solidify the lipid phase and create solid lipid nanoparticles. The resulting samples (BEO-SLNs) were stored at room temperature (13).

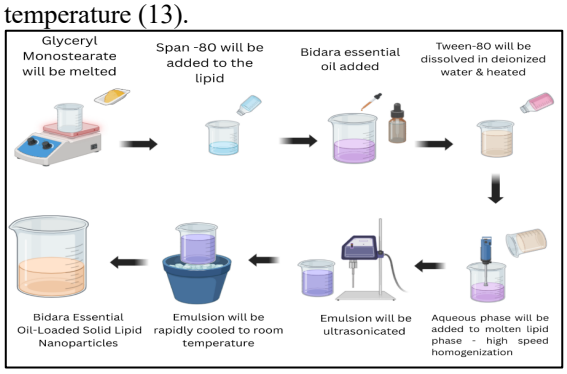


Figure 1 Schematic illustration of the experimental workflow for the preparation of Bidara essential oil-incorporated solid lipid nanoparticles

1.4 Physicochemical characterization of SLNs

1.4.1 Physical appearance

The visual characteristics of the BEO-SLNs were evaluated through visual observation right after they were prepared. Every formulation was examined for colour, consistency, and the occurrence of noticeable instability signs, including aggregation, sedimentation, or phase separation. The observations were recorded to allow for a comparative assessment of the formulations, as visual examination is frequently employed as an initial evaluation of the physical stability of lipid nanoparticle systems (14).

1.4.2 Particle size (PS), polydispersity index (PDI) and zeta potential (ZP)

The particle size, polydispersity index (PDI), and zeta potential of the solid lipid nanoparticles (SLNs) loaded with Bidara essential oil were measured using a Zetasizer Nano-ZS90 device (Malvern Instrument Ltd, Worcestershire, United Kingdom). Dynamic light scattering (DLS) was utilized to assess particle size and PDI, whereas electrophoretic light scattering was applied for the determination of zeta potential. Prior to analysis, the SLN dispersion was diluted at a 1:100 ratio with deionized water to prevent multiple scattering effects(14). Measurements were performed at 25°C using solution with a refractive index of 1.330 and viscosity of 0.8872 cP. For analysing particle size, samples were recorded with a measurement time of 60 seconds. The Z-average diameter represented the average particle size, and the PDI assessed the consistency of particle size distribution (15).

Zeta potential assessments were performed by introducing 1.5 mL of the diluted sample into a transparent disposable zeta cell at 25°C. The electrophoretic mobility of the nanoparticles was measured through 12 measurement runs and the instrument software automatically calculated the zeta potential (16). The values of zeta potential were utilized to evaluate the surface charge and colloidal stability of the SLN formulations.

1.4.3 Oil encapsulation efficiency (EE%) and Loading Capacity (LC%)

Encapsulation efficiency (EE%) and loading capacity (LC%) were evaluated as crucial parameters to assess the effectiveness of solid lipid nanoparticles loaded with Bidara essential oil (BEO-SLNs). Encapsulation efficiency reflects the ratio of Bidara essential oil effectively captured within the lipid matrix (glyceryl monostearate) compared to the overall quantity of oil utilized in the formulation. In contrast, loading capacity indicates the quantity of Bidara essential oil integrated into the nanoparticles compared to the total weight of the nanoparticle system (17). The EE% and LC% of BEO-SLNs were assessed using an indirect UV–Visible spectrophotometric technique. The first step involved was the preparation of stock solution of pure Bidara essential oil in 95% ethanol at a concentration of 1000 µg/mL to guarantee complete solubilization. Subsequently, serial dilutions were then prepared to achieve standard solutions at concentrations of 10, 20, 30, 40, 50, and 60 µg/mL for calibration. These standards were examined with a UV–Visible spectrophotometer (Biobase BK-UV1000G, BIOBASE Group, China) at 225 nm, which relates to the peak absorbance of the essential oil components. The calibration curve exhibited robust linearity and the regression equation derived was describe in the Figure 2.

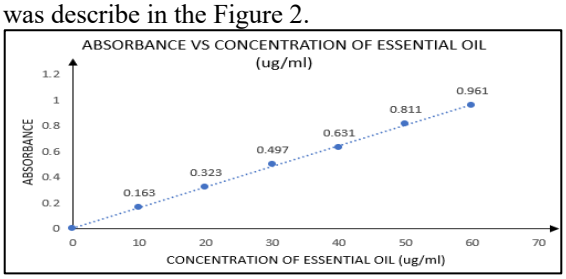


Figure 2: Calibration curve of absorbance versus essential oil concentration

(0-60 µg/mL), showing excellent linearity (y = 0.016x + 0.003, R^2 = 0.9994).

Where y represents absorbance and x represents the concentration of Bidara essential oil (µg/mL), confirming the suitability of the method for quantitative analysis. For sample preparation, 4 mL of BEO-SLNs dispersion underwent centrifugation at 25,000 rpm for 110 minutes at 4°C using an Optima MAX-XP ultracentrifuge (Beckman Coulter Life Sciences Inc., United States) to separate between the nanoparticle-encapsulated oil and the free (unencapsulated) fraction. The solid lipid nanoparticles formed a pellet, whereas the excess oil remained in the supernatant (18). The supernatant that was gathered was gently extracted with a glass pipette to prevent disrupting the pellet and was diluted (1:50) with 95% ethanol to ensure that the absorbance values remained within the linear range of the calibration curve. The absorbance was subsequently recorded in triplicate at 225 nm to enhance analytical precision and consistency (19). The efficiency of encapsulation was determined using this equation.

$$\text{EE\%} = \frac{W_{total} - W_{free}}{W_{total}} \times 100$$

Where W_{total}represents the total Bidara essential oil used in SLN preparation and W_{free}represents the unencapsulated oil detected in the supernatant. All analyses were performed in triplicate, and results were expressed as mean ± standard deviation. The loading capacity was calculated using this equation:

$$\text{LC \%} = \frac{W_{total} - W_{free}}{W_{lipid}} \times 100$$

Where W_{total}denotes the total quantity of Bidara essential oil incorporated into the formulation, W_{free}denotes the quantity of unencapsulated oil remaining in the supernatant and W_{lipid}denotes the quantity of glyceryl monostearate used as the lipid matrix in the SLN formulation.

1.4.4 Morphological Characterization by Scanning Electron Microscopic (SEM)

The morphological characteristics of the optimized BEO-loaded solid lipid nanoparticle (SLN1) formulation were evaluated using scanning electron microscopy (FEI Quanta 450 FEG Scanning Electron Microscopy, Netherlands). A drop of the SLN dispersion was deposited onto a glass coverslip and allowed to air-dry. The dried sample was subsequently sputter-coated with a thin layer of platinum to improve electrical conductivity before imaging. SEM micrographs were acquired at an accelerating voltage of 5.0 kV with a magnification of 20,000× to examine the particle morphology and surface characteristics. (17).

1.5 DPPH radical scavenging activity (RSA)

Bidara (Ziziphus mauritiana) is a medicinal herb well-known for its antioxidant properties. The antioxidant capabilities of Bidara essential oil-loaded solid lipid nanoparticles (BEO-SLNs) were assessed by their effectiveness in neutralizing free radicals through the 2,2-diphenyl-1-picrylhydrazyl (DPPH) assay. This approach relies on the transformation of the stable purple DPPH radical into a yellow product when it accepts hydrogen atoms or electrons from antioxidant substances, indicating the radical scavenging ability of the samples (20). All DPPH solutions were prepared fresh and handled under light-protected environments since the DPPH radical is light-sensitive and can degrade over time, which could affect the accuracy of absorbance readings (21). In brief, 0.5 mL of every test sample, such as BEO-SLNs, blank SLNs (without Bidara essential oil), and ascorbic acid (utilized as a reference standard), was dissolved in ethanol. Every sample was subsequently combined with 1.0 mL of 0.2 mM DPPH solution dissolved in ethanol. The mixtures were thoroughly vortexed and allowed to incubate at room temperature for 30 minutes in the absence of light to avoid light-induced degradation of DPPH.

Following incubation, absorbance readings were taken at 517 nm with a UV-Visible spectrophotometer (Biobase BK-UV1000G, BIOBASE Group, China), with ethanol used as the blank. A reduction in absorbance suggested increased radical scavenging activity as a result of the antioxidant compounds in the samples reducing DPPH radicals (22). The percentage of radical scavenging activity (RSA) was calculated using the following equation:

$$\%RSA = \frac{A_{control} - A_{sample}}{A_{control}} \times 100$$

Where $A_{control}$is the absorbance of the DPPH solution without sample, and $A_{sample}$is the absorbance of the test solution, including BEO-SLNs, blank SLNs, or ascorbic acid. All experiments were conducted in triplicate, and results were expressed as mean ± standard deviation.

1.6 Stability Study

The short-term physical stability of Bidara essential oil-loaded solid lipid nanoparticles (BEO-SLNs) was assessed after a 30-day storage time at a room temperature of 25 ± 2. Recently prepared mixtures were placed in securely sealed glass vials and maintained at a relative humidity of 60%. The formulation's stability was evaluated by observing variations in particle size, polydispersity index (PDI) and zeta potential through dynamic light scattering. Furthermore, the visual characteristics of the formulations were examined for any indications of instability (23).

1.7 Statistical Analysis

Statistical analysis was performed with Microsoft Excel. A one-way analysis of variance (ANOVA) was employed to assess the impact of various solid-to-liquid lipid ratios on particle size, polydispersity index (PDI), and zeta potential throughout the formulation optimization process. Stability over time was evaluated with paired Student's t-tests by comparing the measurements taken on Day 0 and Day 30 in controlled storage conditions (25 ± 2°C). A p-value below 0.05 was deemed statistically significant.

2.0 Results and Discussion

2.1 GC-MS Analysis of Bidara Essential Oil

The analysis of Bidara essential oil's chemical composition was performed using GC-MS, revealing over 10 volatile compounds with varying retention times and peak areas, similar to the data shown in Table 2. The chromatographic analysis demonstrated the predominance of oxygenated monoterpenes and phenolic substances, suggesting that the oil has a chemically reactive volatile component. Multiple compounds were identified within various chemical classes, such as monoterpenoid phenols, monoterpene alcohols, aldehydes, ketones, and derivatives of fatty acids (24). Of all the compounds, carvacrol exhibited the greatest abundance, representing 63.21% of the overall peak area at a retention time of 25.331 min, suggesting that it is the main component of the Bidara essential oil. The mass spectrum of carvacrol featured prominent fragment ions at m/z 102, 60, and 228. Carvacrol is a phenolic monoterpene known for its antimicrobial, antioxidant, anti-inflammatory, and antifungal effects, primarily by disturbing microbial cell membranes and blocking oxidative processes (25).Consistent with prior findings on Ziziphus spina-christi, carvacrol was recognized as a key bioactive component, though its level in this study was markedly elevated (24). Eucalyptol (4.95%), an oxygenated monoterpene, was the second most prevalent compound, followed by a tetradecanoic acid derivative (2.29%), which is a fatty acid ester derivative. Terpenoid aldehydes, such as 3,5-dimethylcyclohex-1-ene-4 carboxaldehyde (1.63%) and 3-cyclohexen-1-carboxaldehyde (0.77%), were identified as well. Minor components primarily included monoterpene alcohols like α-terpineol (0.80%), linalool (0.32%), terpinen-4-ol (0.18%), and borneol (0.06%), alongside camphor (0.29%), a monoterpene ketone, isocyclocitral (0.14%), an oxygenated monoterpene aldehyde, and m-cresol (0.11%), a phenolic substance. Despite being found in relatively small amounts, these substances are recognized for their antimicrobial, antioxidant, and anti-inflammatory effects and might work together to enhance the essential oil's overall biological activity (26).

The predominance of carvacrol, supported by the presence of other bioactive minor constituents, suggests that the Bidara essential oil used in this study is chemically suitable for therapeutic applications and incorporation into nanocarrier systems such as SLNs (27). Furthermore, the chemical profile obtained is consistent with the bioactive composition reported for Bidara essential oils in the literature, thereby supporting the quality and authenticity of the raw material used.

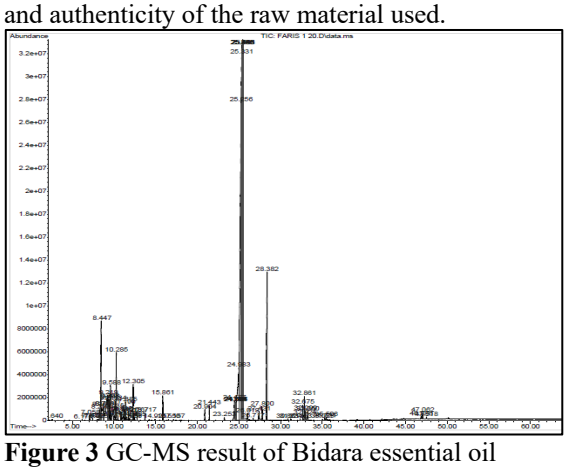


Figure 3 GC-MS result of Bidara essential oil

Table 2 Identified compounds in Bidara Essential oil by GCMS

Compound name	Retention time (min)	%Peak area	m/z (major peaks)	Compound classification

Carvacrol	25.331	63.21	102/60/228	Monoterpenoid phenol
Eucalyptol	24.983	4.95	73/60/129	Monoterpenoid
Tetradecanoic acid	8.447	2.29	81/108/154	Fatty ester
3,5-Dimethylcyclohex-1-ene-4-carboxaldehyde	10.285	1.63	107/67/95	Terpenoid derivative
α-Terpineol	12.305	0.80	59/93/121	Monoterpene alcohol
3-Cyclohexen-1-carboxaldehyde	9.588	0.77	107/67/123	Terpenoid derivatives
7-Octen-2-ol, 2,6-dimethyl-	9.445	0.40	59/55/123	Monoterpenoid
Linalool	10.134	0.32	71/93/55	Monoterpene alcohol
Camphor	11.190	0.29	95/81/108	Monoterpene ketone
Terpinen-4-ol	10.940	0.18	81/121/136	Monoterpene alcohol
Isocyclocitral	10.818	0.14	121/107/81	Monoterpenoid
m-Cresol	9.711	0.11	107/108/77	Phenolic
Borneol	11.486	0.06	95/110/121	Monoterpene alcohol
Terpinen-4-ol	11.956	0.03	71/93/111	Monoterpene alcohol

2.2 Optimization and Characterization of formulations

2.2.1 Particle size (PS) and polydispersity index (PDI)

The average particle size (PS), polydispersity index (PDI), zeta potential (ZP) and encapsulation efficiency (EE%) of Bidara essential oil-loaded SLNs differed across the five formulations with varying solid lipid-to-essential oil ratios. As shown in Table 3, the particle size progressively increased with a higher solid lipid ratio and a lower concentration of essential oil. The particle size of the formulated SLNs was between 87.58 ± 0.86 nm and 98.30 ± 0.31 nm, where SLN1 (5:5 ratio) demonstrated the smallest particle size and SLN5 (8:2 ratio) displayed the largest particle size. The ANOVA assessment showed a significant statistical variation in particle size across the formulated SLNs ($p = 4.86 \times 10^{-10}$). The p-value is significantly lower than the conventional threshold of $p = 0.05$, suggesting that the differences in particle size seen across various solid lipid-to-liquid lipid ratios are extremely significant.

This trend can be attributed to the effect of lipid composition on the viscosity and crystallization characteristics of the internal phase, as an increased solid lipid content improves the viscosity of melted lipids during homogenization. The higher viscosity reduces the effectiveness of droplet breakup under strong shear forces, leading to the formation of larger lipid droplets that solidify into bigger nanoparticles when cooled. Moreover, higher liquid lipid concentrations improve fluidity and emulsification, facilitating better size reduction and leading to smaller nanoparticles (28). Furthermore, the addition of liquid lipid disrupts the rigidity of the solid matrix, reducing its crystallinity. This improved structural disorder allows the lipid core to pack less tightly while cooling, which ultimately facilitates the formation of smaller nanoparticles (29). These findings align with the information shown in Table 3, suggesting that the solid-to-liquid lipid ratio has a considerable impact on SLN particle size by influencing viscosity and crystallization behaviour. However, each formulation exhibited a particle size below 300 nm, which is commonly considered as an indicator of well-formed nanoparticles that demonstrate favourable physical stability and the likelihood of enhanced bioavailability (30).

The PDI values exhibited a non-linear pattern across the formulations, varying from 0.184 ± 0.01 to 0.229 ± 0.01. In general, all formulations showed PDI values under 0.25, signifying satisfactory homogeneity and a relatively narrow particle size distribution (31). The ANOVA findings revealed a $p = 0.00034$, suggesting that changes in lipid composition had a significant impact on the homogeneity of nanoparticles and their particle size distribution.

A small increase in PDI was observed in SLN3 at a 7:3 ratio (0.229 ± 0.01), suggesting reduced uniformity at this lipid composition, possibly associated with insufficient emulsification efficiency and less stable crystallization in nanoparticle formulation. Similar behaviour has been noted in lipid nanoparticle systems by Beloqui et al., where imbalanced solid-to-liquid lipid ratios can lead to heterogeneous nucleation and an increased size distribution because of inconsistent droplet solidification (32).

In contrast, a decrease in PDI was observed in SLN4 and SLN5, with SLN5 (8:2 ratio) showing the lowest PDI (0.184 ± 0.01), indicating the most uniform particle distribution. The reduction in the particle

size distribution may be linked to a higher solid lipid content, which enhances matrix rigidity and promotes uniform crystallization, thereby reducing inconsistencies in particle formation (33). Additionally, enhanced lipid formulation boosts structural stability and reduces variability in nanoparticle systems, resulting in lower PDI values (34).

Table 3 The particle size, PDI and zeta potential of BEO-loaded SLNs with different solid-to-liquid lipid ratios at Day 0 (mean ± SD, N = 3).

Sample	Lipid-to-essential oil ratio	Particle size (nm)	PDI	Zeta potential (mV)
SLN 1	5:5	87.58± 0.86	0.218 ± 0.01	-39.4 ± 4.06
SLN 2	6:4	88.80 ± 0.21	0.218 ± 0.01	-29.6 ± 1.49
SLN 3	7:3	93.86 ± 0.28	0.229 ± 0.01	-32.8 ± 1.07
SLN 4	7.5 :2.5	95.89 ± 0.52	0.192 ± 0.01	-18.6 ± 0.98
SLN 5	8:2	98.30 ± 0.31	0.184 ± 0.01	-17 ± 0.30

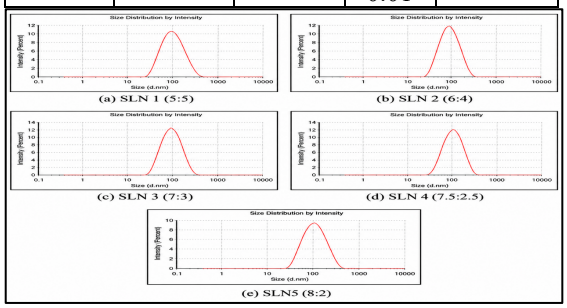


Figure 4 Particle size distribution of BEO-loaded SLNs

2.2.2 Zeta Potential (ZP)

Zeta potential is a key indicator of the surface charge characteristics and colloidal stability of solid lipid nanoparticles (SLNs) (35). The zeta potential values of the SLN formulations ranged from −17.0 ± 0.30 to −39.4 ± 4.06 mV, indicating that all formulations possessed a negative surface charge. In general, zeta potential values exceeding ±30 mV are considered desirable, as the strong electrostatic repulsive forces between particles help minimize aggregation and improve dispersion stability (36). Statistical analysis using one-way ANOVA demonstrated a significant difference between formulations ($p = 4.04 \times 10^{-7}$), indicating that the solid-to-liquid lipid ratio had a significant effect on the zeta potential of the SLNs.

The negative zeta potential values observed cannot be attributed to direct ionic interactions between GMS and the surfactants since glyceryl monostearate (GMS), Span 80, and Tween 80 are non-ionic compounds. The surface charge of the SLNs is probably generated by adsorption of hydroxyl ions (OH^-) and the presence of minor ionized fatty acid species derived from the lipid phase (37). In the process of nanoparticle formation, GMS molecules form the solid lipid matrix, whereas Span 80 and Tween 80 adhere to the lipid-water interface, lowering interfacial tension and stabilizing the nanoparticles (38).

The findings indicated that the formulations with reduced amounts of GMS, specifically SLN 1 to SLN 3, displayed more negative zeta potential values between −29.6 and −39.4 mV, suggesting enhanced electrostatic repulsion among particles and, therefore, improved colloidal stability. Conversely, raising the ratio of GMS in SLN 4 and SLN 5 diminished the zeta potential value to approximately −18 mV. This reduction might be attributed to the creation of a denser lipid matrix, which can restrict the accessibility of charged groups and surfactant molecules at the particle's surface, thus lowering the total surface charge (39).

Previous authors indicate that GMS-based solid lipid nanoparticles usually show moderately negative zeta potential values, aligning with the trend found in the current study. The reduction in zeta potential magnitude with a higher GMS proportion aligns with previous findings that indicated lipid composition and surfactant surface coverage significantly affect the surface charge of SLNs, not just GMS alone. This implies that the lower negative zeta potential seen in SLN 4 and SLN 5 could be due to a more compact lipid matrix and diminished visibility of charged groups on the particle surface, which corresponds with the trends documented in the literature (40).

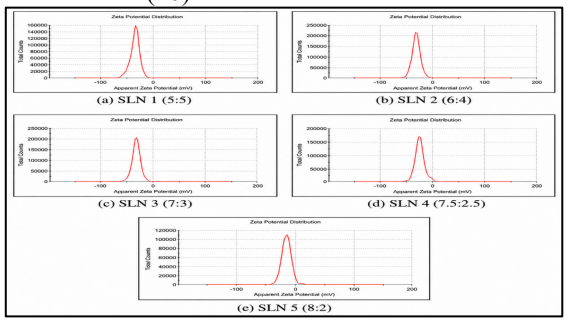


Figure 5 Zeta potential distribution of BEO-loaded SLNs

2.2.3 Encapsulation efficiency (EE%) and Loading capacity (LC%)

Encapsulation Efficiency (EE%) indicates the proportion of the active ingredient (essential oil) that is effectively contained within the solid lipid nanoparticles relative to the total quantity originally utilized in the formulation. A high EE% is preferred to secure adequate therapeutic loading, reduce drug loss during formulation, and facilitate controlled release (41). The encapsulation efficiency for all SLN formulations stayed remarkably high, varying

between 97.34% and 99.54%. SLN 1 (5:5 lipid-to-essential oil ratio) showed the highest EE% (99.54%), while a gradual decline was noted with rising lipid content, hitting 97.34% in SLN 5 (8:2). This minor decline indicates that while the formulations are mostly effective at trapping the essential oil, an increase in solid lipid content might impair the lipid matrix's capacity to incorporate the oil phase properly. This may result from increased crystallinity of the solid lipid, potentially restricting space in the lipid core and encouraging slight release of the encapsulated substance during the solidification of nanoparticles (14). Nonetheless, the uniformly elevated EE% throughout all formulations suggests a robust compatibility between the lipid matrix and essential oil, along with an effective encapsulation process overall.

Loading Capacity (LC%) indicates the quantity of drug effectively contained within the nanoparticles compared to the overall weight of the nanoparticle system. In contrast to EE%, which focuses on the quantity of drug retained, LC% emphasizes the amount of drug incorporated into the ultimate nanoparticle configuration (42). In comparison, the loading capacity exhibited a significant downward trend as lipid content increased, falling from 47.53% in SLN 1 to 18.13% in SLN 5. This decrease suggests that while the total quantity of encapsulated oil stays elevated, the ratio of active compound to total nanoparticle weight significantly declines with increasing lipid concentration. This occurrence can be linked to a dilution effect, where larger quantities of lipid enhance the total mass of the nanoparticles without a corresponding rise in essential oil content. Consequently, formulations featuring reduced lipid ratios exhibited enhanced loading efficiency, with SLN 1 being the most advantageous regarding drug payload capability.

Table 4 The encapsulation efficiency and loading capacity of BEO-loaded SLNs with different solid-to-liquid lipid ratios at Day 0

Sample	Lipid-to-essential oil ratio	Encapsulation efficiency (%)	Loading Capacity (%)
SLN 1	5:5	99.54	47.53
SLN 2	6:4	99.27	37.59
SLN 3	7:3	98.62	27.78
SLN 4	7.5:2.5	98.23	22.96
SLN 5	8:2	97.34	18.13

2.2.4 Morphological Analysis of BEO-SLNs by SEM

The surface morphology of the optimized BEO-loaded solid lipid nanoparticle (SLN1) formulation was examined using scanning electron microscopy (SEM), as shown in Figure 6. The SEM images revealed predominantly spherical to irregularly spherical nanoparticles with a relatively uniform distribution and slight aggregation.

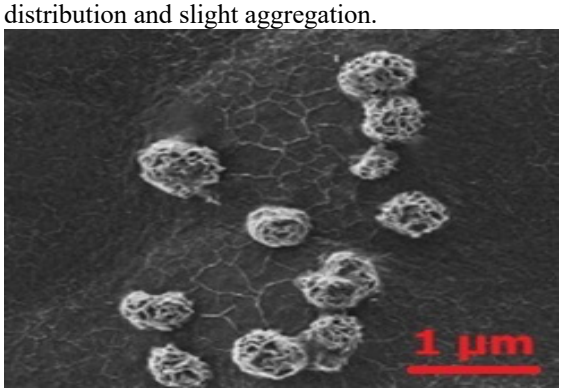


Figure 6 SEM micrographs of BEO-SLNs showing particle morphology at 20000x magnification.

2.3 Antioxidant activity

The antioxidant activity of Bidara essential oil-loaded solid lipid nanoparticles (BEO-SLN) was evaluated using the DPPH free radical scavenging assay, and the results are presented as percentage inhibition. As shown in Table 5, the test formulation (SLN 1) exhibited a high DPPH radical scavenging activity of 72.11 ± 0.1% at the 50 µg/mL concentration. This finding indicates that the incorporation of Bidara essential oil contributes substantially to the antioxidant activity of the SLN system. Although the antioxidant activity of SLN 1 was lower than the standard antioxidant, ascorbic acid (96.6 ± 0.2%), it still demonstrated considerable free radical scavenging potential.

The enhanced antioxidant activity of SLN 1 is primarily due to the presence of carvacrol, the key component found in Bidara essential oil, as indicated in Table 2. Carvacrol is a phenolic monoterpenoid compound recognized for its potent antioxidant characteristics. Its antioxidant action is mainly linked to the existence of a phenolic hydroxyl (-OH) group, which donates hydrogen atoms or electrons to counteract DPPH free radicals, thus stopping free radical chain reactions and averting oxidative harm (43,44).

In summary, the findings indicate that the antioxidant capacity of SLN1 primarily originated from Bidara essential oil. The positive control, ascorbic acid, exhibited nearly total radical scavenging activity, validating its robust antioxidant capacity(45). Although antioxidant activity of *Ziziphus mauritiana* has been demonstrated using the DPPH assay, the available studies mainly involve solvent extracts from leaves, fruit, or seeds rather than the essential oil. Therefore, specific % DPPH scavenging data for *Z. mauritiana* essential oil appear to be insufficiently reported.

Table 5 Antioxidant activity (% scavenging of free radical DPPH) of the test and standard samples (mean ± SD).

Sample	% inhibition
Test (SLN1)	72.11 ± 0.1
Standard (ascorbic acid)	96.6 ± 0.2

2.4 Stability Study

All formulations were chosen for the stability study because of their advantageous initial physicochemical properties, such as appropriate particle size, narrow size distribution, sufficient surface charge and high encapsulation efficiency. The stability of the SLNs was verified by the lack of notable alterations in physical appearance, particle size, PDI, zeta potential and EE% following 30 days of storage at constant temperature. The minor change in particle size implies that the nanoparticles experienced little aggregation or growth, and the consistent PDI values reflect the maintenance of a uniform particle distribution. Zeta potential aids in electrostatic stabilization, while non-ionic surfactants like Tween 80 and Span 80 can also offer steric stabilization, hindering close interactions between particles. Moreover, the slight variations in EE% indicate the successful preservation of the encapsulated essential oil within the lipid matrix, showing minimal leakage during storage. The lack of apparent changes, such as phase separation or precipitation, further verifies the excellent physical and colloidal stability of the SLN formulations

2.4.1 Physical appearance

The newly prepared formulation presented itself as a consistent, non-transparent milky-white dispersion with a smooth and uniform texture. The sample showed no clear indications of phase separation, sedimentation, creaming, or aggregation. The distribution was consistent across the vial, demonstrating effective initial stability and successful particle distribution. The overhead image displayed a uniform creamy-white look without any noticeable lumps, particles, or surface imperfections. The formulation retained a single uniform phase, indicating proper integration of the lipid components and efficient stabilization of the nanoparticles. Following 30 days of storage, the formulation maintained its off-white to milky-white colour, suggesting that there was no notable discoloration or chemical degradation observable to the naked eye. Nevertheless, significant physical alterations were noted in comparison to Day 0. The top section of the vial looked noticeably clearer, suggesting a partial loss of uniformity in the dispersion. Furthermore, deposits sticking to the inner surface of the vial were noted, potentially signifying particle settling and adhesion over time. Regardless of these alterations, there was no noticeable complete phase separation, significant aggregation, or development of large visible clusters. The overhead image continued to display a fairly consistent look, even though minor alterations in opacity and uniformity of dispersion might have taken place. In general, the formulation stayed physically stable but showed indications of a partial decrease in dispersion uniformity after extended storage.

Table 6 The physical appearance of all BEO-loaded SLN formulations on Day 0 & Day 30.

Sample	Solid-to-liquid lipid ratio	Day 0	Day 30
SLN 1	5:5		
SLN 2	6:4		
SLN 3	7:3		
SLN 4	7.5:2.5		

2.4.2 Effect of storage time on particle size and PDI

Particle size analysis was performed to evaluate the effect of storage time (30 days) on the physical stability of the SLN formulations. After 30 days of storage, the particle sizes ranged from 85.11 ± 0.26 nm to 94.89 ± 0.51 nm. SLN 2 exhibited the smallest particle size (85.11 ± 0.26 nm), whereas SLN 5 showed the largest particle size (94.89 ± 0.51 nm). Statistical analysis revealed that the changes in particle size for SLN 1 ($p = 0.158$) and SLN 3 ($p = 0.131$) were not statistically significant ($p > 0.05$), indicating that storage time did not markedly affect the particle size of these formulations. In contrast, significant differences were observed for SLN 2 ($p = 0.004$), SLN 4 ($p = 0.001$), and SLN 5 ($p = 0.001$), suggesting that storage time influenced the particle size of these formulations. The observed differences in particle size may be attributed to physicochemical changes occurring during storage, including polymorphic transformation and lipid matrix rearrangement (46). The lack of notable particle size alterations in SLN 1 and SLN 3 indicates enhanced resistance to particle growth and aggregation during storage (47), reflecting improved physical stability. Additionally, all formulations kept particle sizes under 100 nm after 30 days, indicating that the nanoparticle systems stayed in the desired

nanometric range despite being stored. SLN 1 exhibited the highest stability, displaying a minor particle size and no substantial alteration during storage. The consistent sizes in the formulations might indicate a well-balanced lipid composition and efficient surfactant stabilization (48). Comparable results have been observed in several studies, where SLNs loaded with essential oils exhibited only slight variations in particle size when stored at room temperature, reinforcing the stability noted in the current research (49, 50). In general, all formulations exhibited acceptable physical stability for 30 days, but increased solid lipid content corresponded to larger particle size variations.

The PDI values of the SLN formulations ranged from 0.212 ± 0.01 to 0.250 ± 0.01 after 30 days of storage, indicating a relatively narrow particle size distribution for all formulations. Statistical analysis showed that SLN 1 ($p = 0.179$), SLN 2 ($p = 0.060$), SLN 3 ($p = 0.170$), and SLN 4 ($p = 0.053$) did not exhibit significant changes in PDI during storage ($p > 0.05$), suggesting that the particle size distribution remained relatively stable over time. In contrast, SLN 5 showed a significant change in PDI ($p = 0.030$), indicating a slight alteration in particle distribution during storageRegardless, all PDI values stayed below 0.3, which is typically viewed as signifying a uniform nanoparticle dispersion with excellent consistency. The preservation of low PDI values during the storage period indicates that significant particle aggregation or instability did not take place (51).

The notable alteration in PDI seen for SLN 5 could be linked to lipid recrystallization and polymorphic transitions that take place during storage. Certain studies have indicated that transforming lipid crystals into more stable polymorphic structures can enhance particle heterogeneity and widen the distribution of particle sizes. Nonetheless, the PDI stayed under 0.3, indicating that the formulation preserved satisfactory uniformity and physical stability despite the noted alteration (52). These results are consistent with some previous studies, which reported that SLNs exhibited only minor fluctuations in PDI during storage while remaining within the acceptable range when stabilized with non-ionic surfactants (53, 54).

Table 7. The particle size, PDI, zeta potential, encapsulation efficiency and loading capacity of BEO-loaded SLNs with different solid-to-liquid lipid ratios at Day 30 (mean ± SD, N = 3). (P-values represent paired t-test results comparing Day 0 and Day 30 for each parameter. $p<0.05$ indicates statistical significance)

Sample	Lipid-to-essential oil ratio	Particle size (nm)	Polydispersity index (PDI)	Zeta potential (mV)	Encapsulation efficiency (%)	Loading Capacity (%)
SLN 1	5:5	85.64 ± 0.67 p = 0.158	0.238 ± 0.01 p = 0.179	-32.6 ± 0.66 p= 0.122	99.49	47.52
SLN 2	6:4	85.1 ± 0.26 p = 0.004	0.2423± 0.01 p = 0.06	-28.8 ± 0.45 p = 0.5	99.21	37.57
SLN 3	7:3	93.05 ± 0.30 p = 0.131	0.250 ± 0.01 p = 0.17	-26.3 ± 0.68 p= 0.01	98.54	27.76
SLN 4	7.5 :2.5	93.25 ± 0.45 p = 0.001	0.213 ± 0.01 p = 0.053	-17.9 ± 0.58 p= 0.08	98.10	22.93
SLN 5	8:2	94.89 ± 0.51 p = 0.001	0.212 ± 0.01 p = 0.03	-16.1 ± 0.2 p= 0.004	97.13	18.10

3.4.3 Effect of storage time on zeta potential

Zeta potential analysis was performed to evaluate the effect of storage time (30 days) on the surface charge stability of the SLN formulations. After 30 days of storage, the zeta potential values ranged from −16.1 ± 0.20 mV to −32.6 ± 0.66 mV. SLN 1 exhibited the most negative zeta potential (−32.6 ± 0.66 mV), whereas SLN 5 showed the least negative value (−16.1 ± 0.20 mV). Statistical analysis revealed that the changes in zeta potential for SLN 1 ($p = 0.122$), SLN 2 ($p = 0.500$), and SLN 4 ($p = 0.080$) were not statistically significant ($p > 0.05$), indicating that storage time did not markedly affect

the surface charge of these formulations. In contrast, significant differences were observed for SLN 3 ($p = 0.010$) and SLN 5 ($p = 0.004$), suggesting that storage time influenced the surface charge properties of these formulations. In this research, all formulations showed negative zeta potential values after 30 days of storage, indicating the presence of negatively charged groups on the nanoparticles' surface and aiding in colloidal stability (55).The zeta potential's magnitude declined as the solid lipid content increased, with SLN 1 displaying the most negative value and SLN 5 the least. This trend can be linked to the decreased ratio of essential oil present at the particle surface with the rise in solid lipid concentration, leading to lower surface charge density. Despite notable alterations in SLN 3 and SLN 5, the formulations maintained physical stability, as indicated by their particle size and PDI measurements. The changes noted may relate to reorganization of the lipid matrix or redistribution of surfactants during storage, potentially affecting the surface properties of nanoparticles. Gordillo-Galeano and Mora-Huertas (2021) indicated that alterations in SLN surface characteristics during storage might arise from lipid matrix reorganization and surfactant redistribution, potentially resulting in minor changes in zeta potential while preserving overall colloidal stability(56).

2.4.4 Effect of storage time on encapsulation efficiency and loading capacity

Encapsulation efficiency (EE) was evaluated to determine the ability of the SLN formulations to entrap the essential oil within the lipid matrix. The EE values ranged from 97.13% to 99.49%, indicating excellent encapsulation across all formulations. SLN 1 exhibited the highest EE (99.49%), while SLN 5 showed the lowest EE (97.13%). A slight decreasing trend in EE was observed with increasing lipid-to-essential oil ratio, which may be attributed to reduced accommodation of the oil within the more rigid and highly crystalline lipid matrix, leading to partial expulsion of the active compound during nanoparticle formation (57). Despite this trend, all formulations demonstrated very high EE (>97%), confirming efficient incorporation of the essential oil into the SLN system. Loading capacity (LC) values ranged from 18.10% to 47.52%. SLN 1 showed the highest LC (47.52%), whereas SLN 5 exhibited the lowest LC (18.10%). The observed decrease in LC with increasing lipid content suggests that higher solid lipid proportions reduce the relative amount of essential oil that can be incorporated per unit weight of lipid matrix. This may be due to the increased structural rigidity of the lipid core, which limits the space available for oil entrapment (57). Overall, SLN 1 demonstrated the most favourable balance of high EE and LC, indicating superior drug-loading performance among all formulations.

3.0 Conclusion

This project effectively created Bidara essential oil-loaded solid lipid nanoparticles (BEO-SLNs) through high-shear homogenization and ultrasonication methods. GC-MS analysis revealed carvacrol (63.21%) as the principal bioactive component of Bidara essential oil. The produced BEO-SLNs demonstrated advantageous physicochemical characteristics, such as particle sizes under 100 nm, low PDI values (<0.25), negative zeta potential and high encapsulation efficiency (>97%). SEM analysis further confirmed the successful formation of predominantly spherical to irregularly spherical nanoparticles with rough surface morphology and minimal aggregation, indicating good structural integrity of the formulation. Of all the formulations, SLN1 exhibited the most favourable traits, featuring the smallest particle size, greatest loading capacity, and significant antioxidant activity (72.11 ± 0.01% DPPH inhibition). Stability studies indicated that the formulations retained acceptable physicochemical characteristics following 30 days of storage. The results indicate that BEO-SLNs, especially SLN1, are encouraging nanocarrier systems for enhancing the stability and therapeutic efficacy of Bidara essential oil.

Acknowledgement

The authors would like to express their sincere gratitude to the Faculty of Pharmacy, Universiti Teknologi MARA (UiTM), for the financial support, facilities and technical assistance provided throughout this study.

Conflicts of interests

The authors declare that there are no conflicts of interest.

References

1. Nilofar N, Sinan KI, Dall'Acqua S, Sut S, Uba AI, Etienne OK, et al. Ziziphus mauritiana lam. Bark and leaves: extraction, phytochemical composition, in vitro bioassays and in silico studies. Plants. 2024;13(16).
2. El Maaiden E, El Kharrassi Y, Qarah NA, Essamadi AK, Moustaid K, Nasser B. Genus Ziziphus: A comprehensive review on ethnopharmacological, phytochemical and pharmacological properties. Journal of ethnopharmacology. 2020;259:112950.
3. Hafiz I, Happyana N, Insanu M. Exploring the antioxidant and α-glucosidase inhibitor potential properties across three Ziziphus species: An insight from HPLC data. Journal of Pharmacy and Pharmacognosy Research. 2025;13(5):1385-99.
4. PAULOI L, SALIM R, LIEW KANG C, SUNDANG M, RUSDI NA, MAID M, et al. GC-MS analysis of bioactive compounds in ethanolic extract on different parts of Ziziphus mauritiana. Biodiversitas: Journal of Biological Diversity. 2024;25(10).

5. Tigmeanu CV, Muntean I, Ardelean LC, Roi A, Roi CI, Dinu S, et al. The Therapeutic Role of Plant Extracts in Oral Medicine. 2026.
6. Ni Z-J, Wang X, Shen Y, Thakur K, Han J, Zhang J-G, et al. Recent updates on the chemistry, bioactivities, mode of action, and industrial applications of plant essential oils. Trends in food Science & technology. 2021;110:78-89.
7. Alsayari A, Wahab S. Genus Ziziphus for the treatment of chronic inflammatory diseases. Saudi Journal of Biological Sciences. 2021;28(12):6897-914.
8. Kadi RH, Alqahtani NK, Abdulfattah AM, Alsulaimani F, Basri AM, Algheshairy RM, et al. Anticancer potential of ethanolic sidr leaf extracts against MCF-7 breast cancer cells: phytochemical, nutritional, and antimicrobial profile comparisons of different plant parts. PeerJ. 2025;13:e19858.
9. Silva EFd, Santos FALd, Pires HM, Bastos LM, Ribeiro LNdM. Lipid nanoparticles carrying essential oils for multiple applications as antimicrobials. Pharmaceutics. 2025;17(2):178.
10. Katopodi A, Detsi A. Solid Lipid Nanoparticles and Nanostructured Lipid Carriers of natural products as promising systems for their bioactivity enhancement: The case of essential oils and flavonoids. Colloids and Surfaces A: Physicochemical and Engineering Aspects. 2021;630:127529.
11. Aisha Ashraf AA, Sarfraz R, Farooq Anwar FA, Shahid S, Alkharfy K. Chemical composition and biological activities of leaves of Ziziphus mauritiana L. native to Pakistan. 2015.
12. Wu S, Hatahet T, Bona BL, Lodigiani G, Zhang M, Bombelli FB, Al-Jamal WT. Incorporating Span 80 surfactant into lipid nanocapsules improves their biocompatibility and cellular uptake in B16F10 melanoma cells. International Journal of Pharmaceutics. 2025;672:125358.
13. Kotb EA, El-Shiekh RA, Abd-Elsalam WH, El Sayed NSED, El Tanbouly N, El Senousy AS. Protective potential of frankincense essential oil and its loaded solid lipid nanoparticles against UVB-induced photodamage in rats via MAPK and PI3K/AKT signaling pathways; A promising anti-aging therapy. Plos one. 2023;18(12):e0294067.
14. Sakellari GI, Zafeiri I, Batchelor H, Spyropoulos F. Formulation design, production and characterisation of solid lipid nanoparticles (SLN) and nanostructured lipid carriers (NLC) for the encapsulation of a model hydrophobic active. Food hydrocolloids for health. 2021;1:100024.
15. Nasseri M, Golmohammadzadeh S, Arouiee H, Jaafari MR, Neamati H. Antifungal activity of Zataria multiflora essential oil-loaded solid lipid nanoparticles in-vitro condition. Iranian journal of basic medical sciences. 2016;19(11):1231.
16. da Silva MJF, Rodrigues AM, Costa MCP, Camara AL, Cabral LM, Ricci Junior E, et al. Solid lipid nanoparticles based on babassu oil and copaiba oleoresin: a promising approach for prostate cancer therapy. Nanomaterials. 2024;14(12):1014.
17. Musielak, E., Feliczak-Guzik, A., & Nowak, I. (2022). Optimization of the conditions of solid lipid nanoparticles (SLN) synthesis. *Molecules, 27*(7), 2202. https://doi.org/10.3390/molecules27072202
18. Nasri NAM, Uddin BH, Sarker ZI, Ling CY, Bin LK. Effect of Concentration of Lipid with Surfactant and Ultrasonification Power on the Formation of Naringenin-Loaded Solid Lipid Nanoparticles. Journal of Pharmaceutical Negative Results. 2022;13:104-10.
19. Bustos Araya ME, Ricart AN, Calpena Campmany AC, Prohens R, Miñarro Carmona M. Development and characterization of lyophilized chondroitin sulfate-loaded solid lipid nanoparticles: encapsulation efficiency and stability. Pharmaceutics. 2025;17(1):86.
20. Shahidi F, Samarasinghe A. How to assess antioxidant activity? Advances, limitations, and applications of in vitro, in vivo, and ex vivo approaches. Food Production, Processing and Nutrition. 2025;7(1):1-107.
21. Ratnawaty GJ, Indrawati R, Wahdaniah W, Rakhman KA. AN OVERVIEW OF ADVANCED 2, 2-Diphenyl-1-picrylhydrazyl (DPPH) ANALYSIS TECHNIQUES. Walisongo Journal of Chemistry. 2025;8(2):138-52.
22. Kumar V, Mathela C, Kumar M, Tewari G. Antioxidant potential of essential oils from some Himalayan Asteraceae and Lamiaceae species. Medicine in drug discovery. 2019;1:100004.
23. Khan MFA, Ur. Rehman A, Howari H, Alhodaib A, Ullah F, Mustafa Zu, et al. Hydrogel containing solid lipid nanoparticles loaded with argan oil and simvastatin: Preparation, in vitro and ex vivo assessment. Gels. 2022;8(5):277.
24. Hammad AA, Khaled FA, Hussien SM. GC-MS Characterization of Ziziphus spina-christi Essential Oil and its Antioxidant Efficacy in Rabbit Models. World Journal of Applied Medical Sciences. 2026;3(1):14-8.
25. Ait Benlabchir A, Fikri-Benbrahim K, Moutawalli A, Alanazi MM, Halmoune A, Benkhouili FZ, et al. GC–MS characterization and bioactivity study of Eucalyptus globulus Labill.(Myrtaceae) essential oils and their fractions: antibacterial and antioxidant properties and molecular docking modeling. Pharmaceuticals. 2024;17(11):1552.
26. Salvatori ES, Morgan LV, Ferrarini S, Zilli GA, Rosina A, Almeida MO, et al. Anti-Inflammatory and Antimicrobial Effects of Eucalyptus Spp. Essential Oils: A Potential Valuable Use for an Industry Byproduct. Evidence-Based

Complementary and Alternative Medicine. 2023;2023(1):2582698.
27. De Sousa DP, Damasceno ROS, Amorati R, Elshabrawy HA, De Castro RD, Bezerra DP, et al. Essential oils: Chemistry and pharmacological activities. Biomolecules. 2023;13(7):1144.
28. Khairnar SV, Pagare P, Thakre A, Nambiar AR, Junnuthula V, Abraham MC, et al. Review on the scale-up methods for the preparation of solid lipid nanoparticles. Pharmaceutics. 2022;14(9):1886.
29. Viegas C, Patrício AB, Prata JM, Nadhman A, Chintamaneni PK, Fonte P. Solid lipid nanoparticles vs. nanostructured lipid carriers: a comparative review. Pharmaceutics. 2023;15(6):1593.
30. Mok ZH. The effect of particle size on drug bioavailability in various parts of the body. Pharmaceutical Science Advances. 2024;2:100031.
31. Danaei M, Dehghankhold M, Ataei S, Hasanzadeh Davarani F, Javanmard R, Dokhani A, et al. Impact of particle size and polydispersity index on the clinical applications of lipidic nanocarrier systems. Pharmaceutics. 2018;10(2):57.
32. Zu M, Ma Y, Cannup B, Xie D, Jung Y, Zhang J, et al. Oral delivery of natural active small molecules by polymeric nanoparticles for the treatment of inflammatory bowel diseases. Advanced Drug Delivery Reviews. 2021;176:113887.
33. Bahari LAS, Hamishehkar H. The impact of variables on particle size of solid lipid nanoparticles and nanostructured lipid carriers; a comparative literature review. Advanced pharmaceutical bulletin. 2016;6(2):143.
34. Hou X, Zaks T, Langer R, Dong Y. Lipid nanoparticles for mRNA delivery. Nature Reviews Materials. 2021;6(12):1078-94.
35. Amekyeh H, Billa N. Lyophilized drug-loaded solid lipid nanoparticles formulated with beeswax and theobroma oil. Molecules. 2021;26(4):908.
36. Németh Z, Csóka I, Semnani Jazani R, Sipos B, Haspel H, Kozma G, et al. Quality by design-driven zeta potential optimisation study of liposomes with charge imparting membrane additives. Pharmaceutics. 2022;14(9):1798.
37. Cholakova D, Pagureva N, Hristova M, Tcholakova S. Salt-induced gelation of nonionic sucrose ester dispersions. Journal of Colloid and Interface Science. 2025;693:137610.
38. Ebrahimi HA, Javadzadeh Y, Hamidi M, Jalali MB. Repaglinide-loaded solid lipid nanoparticles: effect of using different surfactants/stabilizers on physicochemical properties of nanoparticles. DARU Journal of Pharmaceutical Sciences. 2015;23(1):46.
39. Musielak E, Feliczak-Guzik A, Nowak I. Optimization of the conditions of solid lipid nanoparticles (SLN) synthesis. Molecules. 2022;27(7):2202.
40. Alamri A, Alqahtani A, Alqahtani T, Al Fatease A, Asiri SA, Gahtani RM, et al. Design, physical characterizations, and biocompatibility of cationic solid lipid nanoparticles in HCT-116 and 16-HBE cells: a preliminary study. Molecules. 2023;28(4):1711.
41. Thuy VN, Van TV, Dao AH, Lee B-J. Nanostructured lipid carriers and their potential applications for versatile drug delivery via oral administration. OpenNano. 2022;8:100064.
42. Herdiana Y, Febrina E, Nurhasanah S, Gozali D, Elamin KM, Wathoni N. Drug loading in chitosan-based nanoparticles. Pharmaceutics. 2024;16(8):1043.
43. de Oliveira AS, Llanes LC, Nunes RJ, Nucci-Martins C, de Souza AS, Palomino-Salcedo DL, et al. Antioxidant activity, molecular docking, quantum studies and in vivo antinociceptive activity of sulfonamides derived from carvacrol. Frontiers in Pharmacology. 2021;12:788850.
44. Pérez-Rosés R, Risco E, Vila R, Peñalver P, Cañigueral S. Antioxidant activity of Tween-20 and Tween-80 evaluated through different in-vitro tests. Journal of Pharmacy and Pharmacology. 2015;67(5):666-72.
45. Nakanishi I, Shoji Y, Ohkubo K, Fukuhara K, Ozawa T, Matsumoto K-i, Fukuzumi S. Effects of reaction environments on radical-scavenging mechanisms of ascorbic acid. Journal of Clinical Biochemistry and Nutrition. 2021;68(2):116-22.
46. Subroto E, Andoyo R, Indiarto R. Solid lipid nanoparticles: review of the current research on encapsulation and delivery systems for active and antioxidant compounds. Antioxidants. 2023;12(3):633.
47. Stahl MA, Lüdtke FL, Grimaldi R, Gigante ML, Ribeiro APB. Characterization and stability of solid lipid nanoparticles produced from different fully hydrogenated oils. Food Research International. 2024;176:113821.
48. Hoseini B, Jaafari MR, Golabpour A, Momtazi-Borojeni AA, Karimi M, Eslami S. Application of ensemble machine learning approach to assess the factors affecting size and polydispersity index of liposomal nanoparticles. Scientific Reports. 2023;13(1):18012.
49. Ribeiro LNdM, De Paula E, Rossi DA, Martins FA, de Melo RT, Monteiro GP, et al. Nanocarriers from natural lipids with in vitro activity against Campylobacter jejuni. Frontiers in cellular and infection microbiology. 2021;10:571040.
50. Carvalho FVd, Ribeiro LNdM, Moura LDd, Rodrigues da Silva GH, Mitsutake H, Mendonça TC, et al. Docetaxel loaded in copaiba oil-nanostructured lipid carriers as a promising DDS for breast cancer treatment. Molecules. 2022;27(24):8838.

51. Muccelin VV, Vellozo OC, Valente TL, Pupe CG, Carvalho EL, Detoni CB. Stability-Focused Nanoparticle Development: Applying Particle Size Stability as a Response Factor in the Design of Experiments. ACS omega. 2025;10(25):26546-50.
52. Salminen H, Kasapoğlu KN, Özçelik B, Weiss J. Stabilization of solid lipid nanoparticles with glycyrrhizin. European Food Research and Technology. 2023;249(3):787-98.
53. Cassayre M, Oline A, Orneto C, Wafo E, Abou L, Altié A, et al. Optimization of solid lipid nanoparticle formulation for cosmetic application using design of experiments, PART II: Physical characterization and in vitro skin permeation for Sesamol skin delivery. Cosmetics. 2024;11(4):120.
54. Jamous YF, Altwaijry NA, Saleem MT, Alrayes AF, Albishi SM, Almeshari MA. Formulation and characterization of solid lipid nanoparticles loaded with troxerutin. Processes. 2023;11(10):3039.
55. Mohammadi-Jam S, Waters KE, Greenwood RW. A review of zeta potential measurements using electroacoustics. Advances in Colloid and Interface Science. 2022;309:102778.
56. Gordillo-Galeano A, Mora-Huertas CE. Hydrodynamic diameter and zeta potential of nanostructured lipid carriers: Emphasizing some parameters for correct measurements. Colloids and surfaces A: Physicochemical and engineering aspects. 2021;620:126610.
57. Himed L, Merniz S, Djerri R, Akachat B, Boussioud H, Berkati A, et al. Encapsulation Strategies for Lemon Essential Oil in Lipid-Based Food Systems: Recent Advances and Applications in Oxidative Stability. Foods. 2026;15(5):950.